Energy Informatics

RESEARCH Open Access

Simmering tensions on the Russia–Ukraine border and natural gas futures prices: identifying the impact using new hybrid GARCH

Chikashi Tsuji[1*]

*Correspondence:
ctsuji001u@g.chuo-u.ac.jp

[1] Graduate School of Economics, Chuo University, Tokyo, Japan

Abstract

Focusing on the Russia–Ukraine war, this paper investigates natural gas futures volatilities. Applying several hybrid GARCH and EGARCH models, which innovatively incorporate both fat-tailed distribution errors and structural breaks, we derive the following new evidence. First, our hybrid modeling approach is effective in timely capturing the natural gas futures volatility spike when tensions simmered on the Russia–Ukraine border. Second, the hybrid modeling approach is effective for not only GARCH modeling but also EGARCH modeling. Third, the volatility estimates from our hybrid models have predictive power for the volatilities of nonhybrid models. Fourth, the volatility estimates from the nonhybrid models lag behind the volatilities of our hybrid models.

Keywords: Artificial intelligence, EGARCH, EGARCH–X, GARCH, GARCH–X, GED error, Natural gas futures, Structural break, Volatility

Introduction

On January 27, 2022, Cable News Network (CNN) reported that the US Pentagon said Russian buildup had increased "in the last 24 hours" near Ukraine, and tensions on the Russia–Ukraine border simmered (CNN 2022). When we examine the data, we can see that the Russia–Ukraine war had a significant impact on natural gas futures prices due to concerns about the imbalance in natural gas supply and demand.

In recent literature on natural gas, there have been studies on (*i*) natural gas hydrates as a new and clean energy source (e.g., Koh et al. 2016; Ding et al. 2017; Liu et al. 2018b; Xu et al. 2018a, 2018b; Gambelli and Rossi 2019; Tupsakhare and Castaldi 2019; Zhu et al. 2020), (*ii*) substitutes for natural gas production through CO methanation (e.g., Bian et al. 2016; Tao et al. 2016, 2017; Liu et al. 2018a; Zhang et al. 2020; Cisneros et al. 2021), (*iii*) sustainable hydrogen production through enhanced natural gas production (e.g., Sanusi and Mokheimer 2019; Guban et al. 2020; Ji and Wang 2021; Olabi et al. 2021; Qureshi et al. 2022; Younas et al. 2022), (*iv*) mercury control technologies in natural gas (e.g., Pontes et al. 2014; Koulocheris et al. 2018; Chalkidis et al. 2019; Wang et al. 2020; Zhou et al. 2020; Koulocheris et al. 2023; Shen et al. 2023), (*v*) the impact of natural

gas and hydrogen properties on internal combustion engine performance (e.g., Wei and Geng 2016; Thiruvengadam et al. 2018; Tutak et al. 2020; Kim et al. 2021; Wang et al. 2021; Chen et al. 2023; Li et al. 2023), and (*vi*) market prices for natural gas (e.g., Wang et al. 2022; Akcora and Kocaaslan 2023; Dastan 2023; Liu et al. 2023; Su et al. 2023; Mensi et al. 2024).

Reviewing the recent studies on market prices for natural gas, Wang et al. (2022) investigated the volatilities of oil rents and natural gas rents. Akcora and Kocaaslan (2023) examined the price bubbles in European natural gas markets. Dastan (2023) investigated the Turkish natural gas market during the supply disruptions that occurred in early 2022. Further, Liu et al. (2023) analyzed the impacts of oil and natural gas prices on China's carbon efficiency. Su et al. (2023) examined whether there were multiple bubbles in the European natural gas market. Mensi et al. (2024) investigated the connectedness between bond, oil, and natural gas prices. Although not focused on natural gas, many studies have argued for the importance of analyzing market prices for energy (e.g., Ju et al. 2014; Tsuji 2018, 2020; van Eyden et al. 2019; Dutta et al. 2021; Puig-Gamero et al. 2021; Jingjian et al. 2023).

Given this and considering the importance of actual natural gas market prices, our current analysis focuses on the impact of the the Russia–Ukraine war on natural gas futures prices. We suggest that in doing such new analysis, it is vital to incorporate fat-tailed distributions and structural breaks. However, in existing studies, although either fat-tailed distributions (e.g., Geweke 1993; Fan et al. 2008) or structural breaks (e.g., Wang and Moore 2009; Malik 2022) are considered, both components are not incorporated into a single model simultaneously. Therefore, our approach of newly considering and incorporating both in this study fills a research gap left by existing literature.

Hence, we examine natural gas futures volatilities of the period around the Russian invasion of Ukraine, with a particular focus on the impact of simmering tensions on the Russia–Ukraine border on natural gas futures volatilities, especially because at that time, a very large volatility spike was observed. We consider that this spike was due to heightened concerns about the imbalance in natural gas supply and demand, particularly at that time.

Our research questions are as follows. "How do we well capture the natural gas futures volatility spike when the tensions simmered on the Russia–Ukraine border by considering both fat-tailed errors and structural breaks as hybrid models?" and "What is the beneficial characteristic of the volatility estimated by our superior hybrid models?" To clarify these matters is the goal of this study. For this purpose, we develop new hybrid generalized autoregressive conditional heteroscedasticity (GARCH) models, which incorporate not only fat-tailed distribution errors but also structural breaks. To the best of our knowledge, no existing study has analyzed the points raised in our research questions mentioned above.

As a result of our careful examinations applying four new hybrid models, i.e., the autoregressive (AR) mean Student's t (T) distribution error and structural break (SB) incorporated GARCH model (hereinafter, the AR–T–SB–GARCH model), the AR–generalized error distribution (GED)–SB–GARCH model (hereinafter, the AR–GED–SB–GARCH model), the AR–T–SB–exponential GARCH (EGARCH) model (hereinafter, the

AR–T–SB–EGARCH model), and the AR–GED–SB–EGARCH model, we have uncovered the following findings as new contributions to this topic area.

First, we reveal that it was not when Russia invaded Ukraine in February 2022, but rather when tensions on the Russia–Ukraine border simmered in January 2022, that the Russia–Ukraine war had the most impact on natural gas futures prices. Second, we clarify that our hybrid models, which incorporate both fat-tailed distribution errors—either Student's t distribution or GED errors—and structural breaks, are effective to capture the natural gas futures volatility jump in a timely manner when tensions on the Russia–Ukraine border simmered.

Third, we also reveal that our hybrid modeling approach—incorporating both fat-tailed errors and structural breaks—is effective not only in GARCH but also in EGARCH modeling. This proves the robustness of our hybrid approach for modeling natural gas futures volatilities. Fourth, we further uncover that the volatility estimates from our hybrid models of the AR–T–SB–GARCH and the AR–GED–SB–GARCH models have predictive power for the volatilities of nonhybrid versions of the AR–T–GARCH and AR–GED–GARCH models. We consider that because of this characteristic, our two hybrid GARCH models well capture the natural gas futures volatility spike when the tensions on the Russia–Ukraine border simmered.

Fifth, we further reveal that the volatility estimates from our exponential-form hybrid AR–T–SB–EGARCH and AR–GED–SB–EGARCH models also have forecast power for the volatilities of nonhybrid AR–T–EGARCH and AR–GED–EGARCH models. This indicates the robustness of both (*i*) the volatility predictive power and (*ii*) our perspective that because of this timely characteristic of the volatility estimates from our hybrid models, our four hybrid GARCH and EGARCH models well capture the jump in natural gas futures volatility when tensions on the Russia–Ukraine border simmered.

Sixth, we suggest that our new evidence of the predictive power of hybrid models for the volatilities of nonhybrid models means that the volatilities from the nonhybrid models lag behind those of the hybrid models. We consider that because of this characteristic, the nonhybrid models are inferior to hybrid models in capturing the natural gas futures volatility spike in a timely manner when tensions on the Russia–Ukraine border simmered. Seventh, in addition to the points mentioned above, we also derive many valuable interpretations, implications, and innovative perspectives for future energy informatics research and risk management in the energy industries through the use of artificial intelligence (AI). This emphasizes the significance of our work.

The remainder of the paper is organized as follows. Section "Data and the characteristics" details the data and the characteristics, Section "Hybrid GARCH models" presents our hybrid GARCH models, and Section "Why are hybrid GARCHs effective?" tests the predictive power of their volatility estimates. Afterwards, Section "Hybrid EGARCH models" provides our hybrid EGARCH models, Section "Why are hybrid EGARCHs effective?" examines the predictive power of their volatility estimates, and Section "Implications and perspectives" provides the implications and our innovative perspectives. Finally, Section "Contributions and conclusions" concludes the paper.

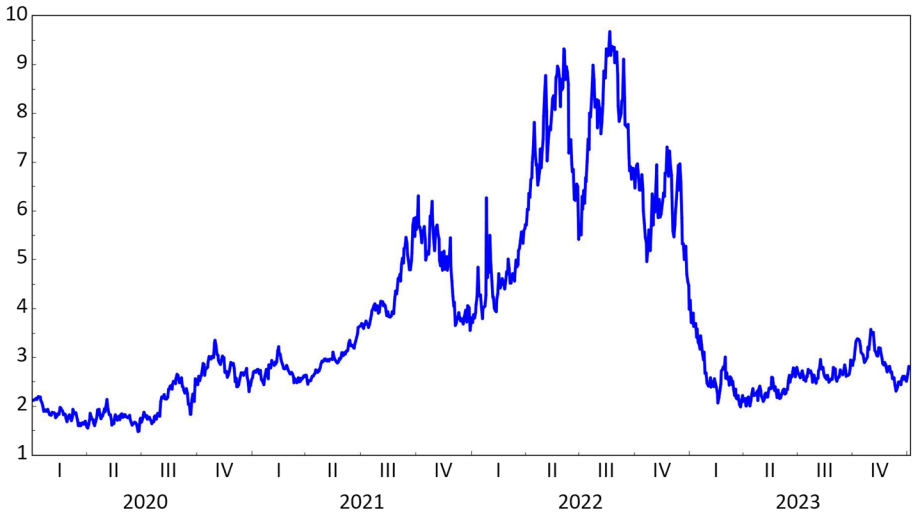

Fig. 1 Daily price evolution of natural gas futures, January 2020 to January 2024. Natural gas futures prices in US dollars

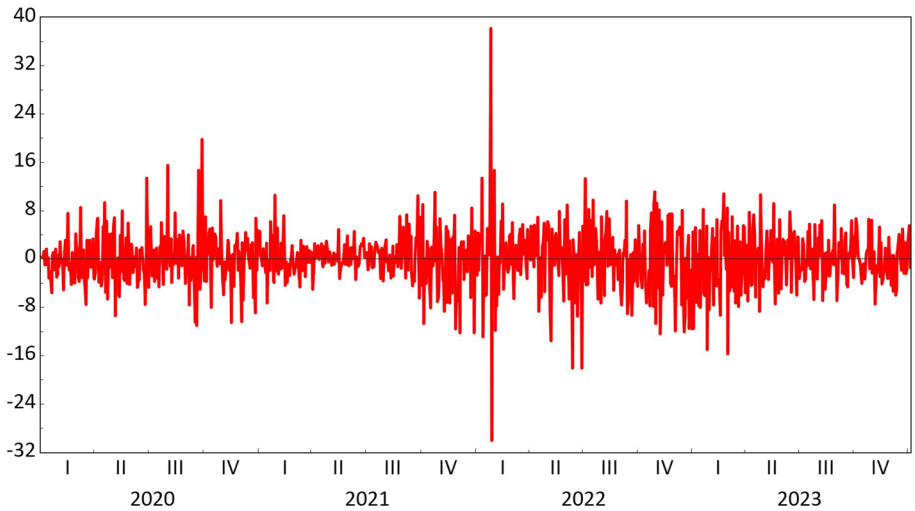

Fig. 2 Daily return evolution of natural gas futures, January 2020 to January 2024. Natural gas futures returns in percent

Data and the characteristics

This study uses the natural gas futures price data from the New York Mercantile Exchange. Using the price series, denoted p^{NG}, we compute the daily log-difference percentage return series as $dlr_t^{NG} = \ln(p_t^{NG}/p_{t-1}^{NG}) \times 100$. To examine the effectiveness of our hybrid models described later for capturing the natural gas futures price fluctuations during the Russian invasion of Ukraine, we analyze the returns, dlr_t^{NG}, from January 3, 2020, to January 5, 2024. We note that this sample period also means the post-COVID-19 outbreak period.

Figures 1 and 2 plot the price and return evolution of the natural gas futures, respectively. From these figures, we can see that before the Russian invasion of Ukraine in

Table 1 Summary statistics for natural gas futures returns, January 2020 to January 2024

	Mean	Median	Minimum
Statistic value	0.027	0.079	−30.048
	Maximum	Standard deviation	Skewness
Statistic value	38.173	4.700	0.151
	Excess kurtosis	JB	ADF
Statistic value	6.452	1,757.679 (0.000)	−35.264 (0.000)

JB: Jarque–Bera statistic; ADF: augmented Dickey–Fuller test statistic. *p*-values are in parentheses

Table 2 Structural break points for natural gas futures return residuals, January 2020 to January 2024

Number	Data point	Date
1	179	September 16, 2020
2	188	September 29, 2020
3	285	February 18, 2021
4	417	August 25, 2021
5	523	January 26, 2022
6	531	February 7, 2022
7	838	April 27, 2023

Break points are identified by the ICSS algorithm

February 2022, natural gas futures prices had jumped (Fig. 1), and the returns largely and sharply fluctuated (Fig. 2). Referring to the return data, the largest return jump took place on January 27, 2022, which was when tensions on the Russia–Ukraine border simmered as discussed.

Table 1 provides summary statistics of the daily natural gas futures returns. The high kurtosis values and large Jarque–Bera statistics in this period indicate that it is meaningful to employ non-normal distribution errors in quantitative models like our present analysis. Moreover, the augmented Dickey–Fuller test statistic indicates that natural gas futures returns are stationary, suggesting that applying GARCH models like ours is applicable.

Furthermore, as Fig. 2 also indicates, there clearly exist structural breaks in natural gas futures returns. Hence, we investigated and identified the structural break points using the iterated cumulative sums of squares (ICSS) algorithm (Inclán and Tiao 1994). We stress that this ICSS algorithm is a very effective algorithm for identifying structural breaks in time series data (e.g., Wang and Moore 2009; Malik 2022). More precisely, as the Bayesian information criterion (BIC) suggests the appropriate autoregressive lag order for the natural gas futures returns is one, we estimate the regression, $dlr_t^{NG} = \mu + \kappa dlr_{t-1}^{NG} + \tau_t$, and identify the structural break points in the return residuals, τ_t.

As shown in Table 2, we find that the number of break points for our analysis period is seven. We also show these break points with the bands of ± 3 standard deviations of the return residuals in Fig. 3. We consider that this figure clearly indicates the importance of taking structural breaks into consideration to analyze the impact of the Russia–Ukraine war on natural gas futures prices.

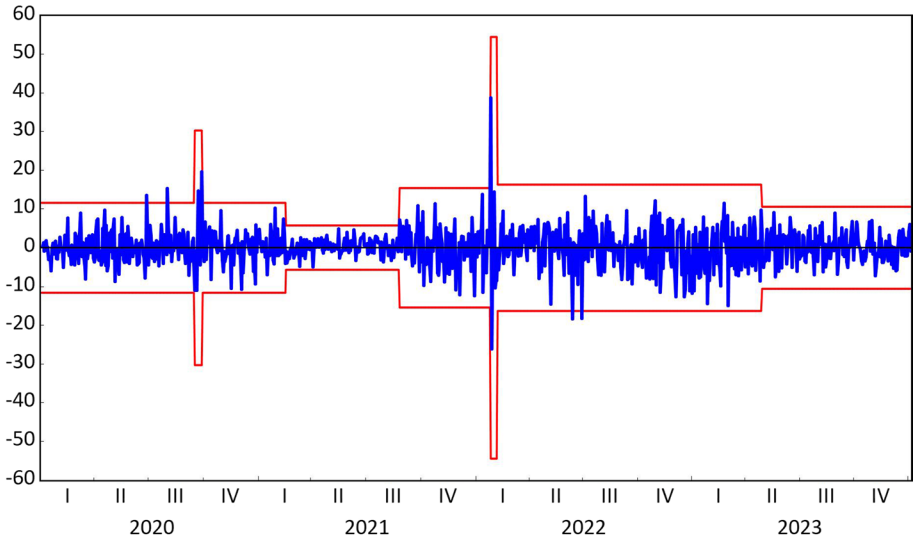

Fig. 3 Structural breaks in natural gas futures return residuals. Bands of ±3 standard deviations and change points identified by the ICSS algorithm

Hybrid GARCH models

Model constructions

This section constructs our hybrid volatility estimation models. Note that we use 'hybrid' to refer to the incorporation of both non-normal fat-tailed errors and structural breaks throughout this study. Due to the non-normality of natural gas futures returns shown in Table 1, we employ either Student's t distribution or GED errors in our models. This is because existing literature suggests the effectiveness of modeling fat-tailed asset returns using Student's t or the GED distribution (e.g., Geweke 1993; Fan et al. 2008). As stated, the BIC suggests the adequate autoregressive lag order for natural gas futures returns is one, and we thus include only the first autoregressive variable in the mean equations of all our models.

Accordingly, the base models used to construct our hybrid GARCH models are the following AR–T–GARCH and AR–GED–GARCH models:

$$\begin{aligned} dlr_t^{NG} &= \mu + \kappa dlr_{t-1}^{NG} + \tau_{t,t}, \\ h_{t,t} &= \psi + \chi \tau_{t,t-1}^2 + \xi h_{t,t-1}, \end{aligned} \tag{1}$$

and

$$\begin{aligned} dlr_t^{NG} &= \mu + \kappa dlr_{t-1}^{NG} + \tau_{g,t}, \\ h_{g,t} &= \psi + \chi \tau_{g,t-1}^2 + \xi h_{g,t-1}, \end{aligned} \tag{2}$$

where dlr_t^{NG} denotes the return of natural gas futures at time t; $\tau_{t,t}$ ($\tau_{g,t}$) denotes the Student's t distribution (GED) errors at time t with ν (k) being the distribution shape parameter; and $h_{t,t}$ ($h_{g,t}$) is the variance to be estimated by model (1) (model (2)) at time t. In addition, μ denotes the mean equation intercept; κ denotes the autoregressive term coefficient; ψ is the variance equation intercept; χ is the ARCH-term coefficient; and ξ is the GARCH-term coefficient.

As the next step, we construct two hybrid GARCH models by including structural break effects into models (1) and (2). Namely, our hybrid GARCH models are the following AR–T–SB–GARCH and AR–GED–SB–GARCH models:

$$\begin{aligned} dlr_t^{NG} &= \mu + \kappa dlr_{t-1}^{NG} + \tau_{tsb,t}, \\ h_{tsb,t} &= \psi + \chi \tau_{tsb,t-1}^2 + \xi h_{tsb,t-1} + \sum_{i=1}^{n} \phi_i D_{i,t}^{SB}, \end{aligned} \tag{3}$$

and

$$\begin{aligned} dlr_t^{NG} &= \mu + \kappa dlr_{t-1}^{NG} + \tau_{gsb,t}, \\ h_{gsb,t} &= \psi + \chi \tau_{gsb,t-1}^2 + \xi h_{gsb,t-1} + \sum_{i=1}^{n} \phi_i D_{i,t}^{SB}, \end{aligned} \tag{4}$$

where $\tau_{tsb,t}$ ($\tau_{gsb,t}$) denotes the Student's t distribution (GED) errors in model (3) (model (4)) at time t; and $h_{tsb,t}$ ($h_{gsb,t}$) is the variance to be estimated by model (3) (model (4)) at time t.

In addition, $D_{i,t}^{SB}$ denotes the i-th structural break dummy variable, n is the number of structural breaks, and ϕ_i is the i-th structural break dummy variable's coefficient. The i-th structural break dummy variable takes a value of zero until the break point identified for the return residuals by the ICSS algorithm, and one thereafter. This study employs the ICSS algorithm because existing studies suggest its effectiveness in capturing structural breaks in asset returns (e.g., Wang and Moore 2009; Malik 2022). For details of the ICSS algorithm, see Inclán and Tiao (1994). Note that including the parameters of the non-normal fat-tailed distributions, ν and k, the other notations of models (3) and (4) described above are the same as those of models (1)–(2).

Verifications

Table 3 provides the estimation results of models (1)–(4). We note that all model parameters are estimated using the maximum likelihood method throughout the paper. Panels A–D present that all the model parameters including the shape parameters of the fat-tailed distribution errors are generally well estimated. In addition, as Panels B and D show, most of the coefficients of our structural break dummy variables—ϕ_1 to ϕ_7—are statistically significant.

It is noteworthy that when incorporating structural breaks, the ARCH effect disappears (The significant coefficients, χ, in Panels A and C of Table 3 become insignificant in Panels B and D.) and the GARCH effect is weakened (The significant values of the coefficients, ξ, in Panels A and C of Table 3 become smaller in Panels B and D.). This also indicates the effectiveness of structural breaks in explaining the evolution of natural gas futures volatilities.

We also conduct likelihood ratio (LR) tests to compare the performance of models (1)–(4) and present the results in Table 4. As shown in Table 4, the null hypotheses—the AR–GARCH model, which has normal distribution errors, is superior to the AR–T–GARCH model (Panel A), the AR–T–GARCH model is superior to the AR–T–SB–GARCH model (Panel B), the AR–GARCH model is superior to the AR–GED–GARCH model

Table 3 Estimation results for hybrid GARCH models

Panel A. AR–T–GARCH			**Panel B. AR–T–SB–GARCH**		
Coefficients	**Estimates**	***p*-value**	**Coefficients**	**Estimates**	***p*-value**
Mean equations					
μ	0.148	0.195	μ	0.112	0.312
κ	−0.033	0.305	κ	−0.032	0.305
Variance equations					
ψ	0.159	0.149	ψ	7.879***	0.002
χ	0.079***	0.000	χ	−0.002	0.948
ξ	0.918***	0.000	ξ	0.457***	0.005
			ϕ_1	50.923	0.145
			ϕ_2	−50.575	0.147
			ϕ_3	−6.264***	0.008
			ϕ_4	12.491***	0.003
			ϕ_5	154.596*	0.098
			ϕ_6	−152.890	0.101
			ϕ_7	−9.362***	0.003
ν	7.386***	0.000	ν	27.037	0.162
LL	−2886.016		LL	−2845.073	
Panel C. AR–GED–GARCH			**Panel D. AR–GED–SB–GARCH**		
Coefficients	**Estimates**	***p*-value**	**Coefficients**	**Estimates**	***p*-value**
Mean equations					
μ	0.167	0.133	μ	0.112	0.307
κ	−0.034	0.254	κ	−0.033	0.287
Variance equations					
ψ	0.143	0.167	ψ	8.034***	0.001
χ	0.079***	0.000	χ	−0.007	0.799
ξ	0.919***	0.000	ξ	0.462***	0.003
			ϕ_1	50.372	0.133
			ϕ_2	−50.163	0.134
			ϕ_3	−6.295***	0.005
			ϕ_4	12.461***	0.002
			ϕ_5	155.468*	0.077
			ϕ_6	−153.715*	0.079
			ϕ_7	−9.461***	0.002
k	1.404***	0.000	k	1.086***	0.000
LL	−2891.467		LL	−2845.453	

LL: log-likelihood value. *** and * denote the 1% and 10% significance levels, respectively

(Panel C), and the AR–GED–GARCH model is superior to the AR–GED–SB–GARCH model (Panel D)—are all strongly rejected.

Moreover, the values of the Akaike's information criterion (AIC) for models (1)–(4) are 5,784.032, 5,794.934, 5,716.146, and 5,716.906, respectively. That is, the LR test results and the AIC values clearly indicate the superiority of our hybrid models, the AR–T–SB–GARCH model and the AR–GED–SB–GARCH model, and demonstrate the effectiveness for taking both non-normal fat-tail errors and structural breaks into account in our analysis for natural gas futures volatilities.

Table 4 LR tests for GARCH model discrimination

Panel A. AR–GARCH vs. AR–T–GARCH	
$\chi^2(1)$	47.208***
p-value	0.000
Panel B. AR–T–GARCH vs. AR–T–SB–GARCH	
$\chi^2(7)$	81.886***
p-value	0.000
Panel C. AR–GARCH vs. AR–GED–GARCH	
$\chi^2(1)$	36.306***
p-value	0.000
Panel D. AR–GED–GARCH vs. AR–GED–SB–GARCH	
$\chi^2(7)$	92.029 ***
p-value	0.000

*** denotes the 1% significance level. The test statistic follows a $\chi^2(n)$ distribution with *n* degrees of freedom. The null hypotheses are: the AR–GARCH model is superior to the AR–T–GARCH model (Panel A); the AR–T–GARCH model is superior to the AR–T–SB–GARCH model (Panel B); the AR–GARCH model is superior to the AR–GED–GARCH model (Panel C); the AR–GED–GARCH model is superior to the AR–GED–SB–GARCH model (Panel D). AR–GARCH model has normal distribution errors

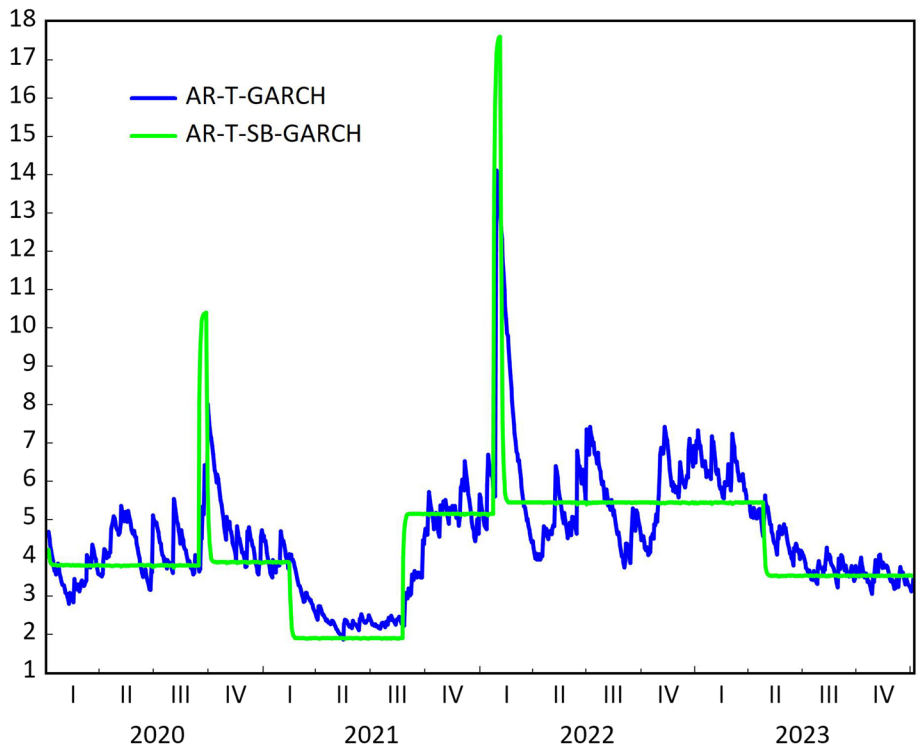

Fig. 4 Estimated daily volatilities from AR–T–GARCH and AR–T–SB–GARCH models

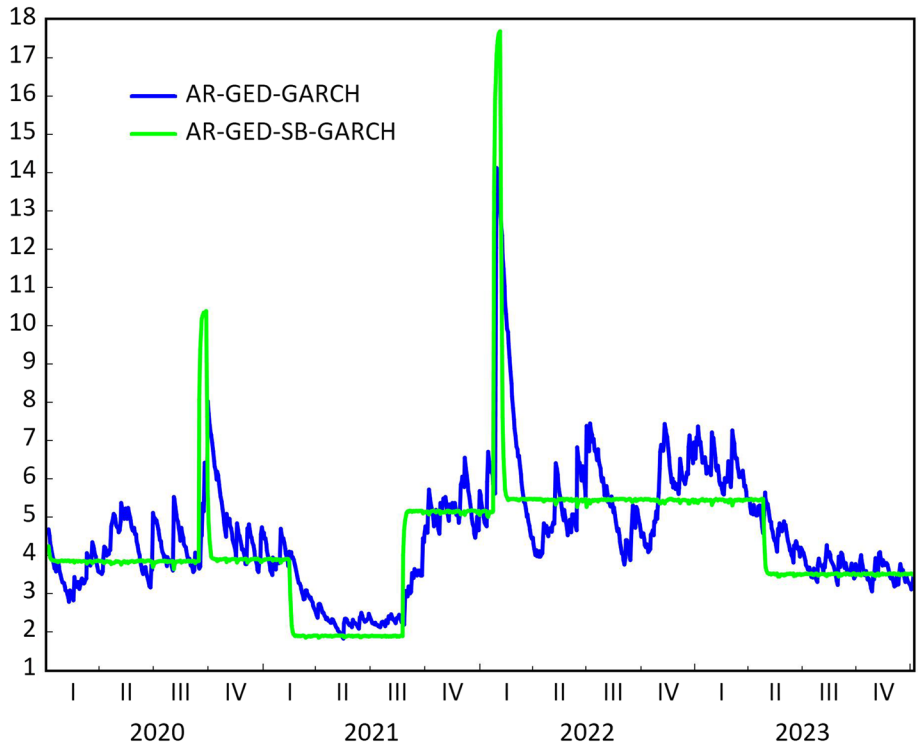

Fig. 5 Estimated daily volatilities from AR–GED–GARCH and AR–GED–SB–GARCH models

Why are hybrid GARCHs effective?

This section considers why our hybrid GARCH models are effective. For this purpose, we plot the volatility estimates in Figs. 4 and 5 to compare our model estimations. Specifically, Fig. 4 illustrates the volatility estimates from the AR–T–GARCH model with those from the AR–T–SB–GARCH model, and Fig. 5 presents the volatility estimates from the AR–GED–GARCH model with those from the AR–GED–SB–GARCH model.

From Figs. 4 and 5, we can see that when volatilities spike, the volatility estimates from the AR–T–SB–GARCH and the AR–GED–SB–GARCH models lead the volatility estimates from the AR–T–GARCH and the AR–GED–GARCH models, respectively. Considering this and clarifying why our hybrid GARCH models are effective, we test below whether our hybrid model volatility estimates have predictive power for the volatilities of the nonhybrid models.

Testing models

This section examines the predictive power of the hybrid model volatility estimates for the nonhybrid model volatilities (precisely, variances). Specifically, to test the forecast power of the volatility estimates from the AR–T–SB–GARCH model (3), we first use the following AR–T–GARCH–X model with $\sqrt{\hat{h}_{tsb,t-1}}$ and the AR–GED–GARCH–X model with $\sqrt{\hat{h}_{tsb,t-1}}$:

$$\begin{aligned} dlr_t^{NG} &= \mu + \kappa dlr_{t-1}^{NG} + \tau_{t,t}, \\ h_{t,t} &= \psi + \chi \tau_{t,t-1}^2 + \xi h_{t,t-1} + \lambda \sqrt{\hat{h}_{tsb,t-1}}, \end{aligned} \tag{5}$$

and

$$\begin{aligned} dlr_t^{NG} &= \mu + \kappa dlr_{t-1}^{NG} + \tau_{g,t}, \\ h_{g,t} &= \psi + \chi \tau_{g,t-1}^2 + \xi h_{g,t-1} + \lambda \sqrt{\hat{h}_{tsb,t-1}}, \end{aligned} \tag{6}$$

where $\sqrt{\hat{h}_{tsb,t-1}}$ denotes the one-day lagged volatility estimates from our hybrid model (3), and λ is the coefficient. Hence, the statistically significant positive λ values indicate the predictive power of the volatility estimates from our hybrid model, the AR–T–SB–GARCH model (3). Note that the other notations of models (5)–(6) are the same as those of models (1)–(2).

Moreover, to test the forecast power of the volatility estimates from the AR–GED–SB–GARCH model (4) for the nonhybrid model volatilities (variances), we use the following AR–T–GARCH–X model with $\sqrt{\hat{h}_{gsb,t-1}}$ and the AR–GED–GARCH–X model with $\sqrt{\hat{h}_{gsb,t-1}}$:

$$\begin{aligned} dlr_t^{NG} &= \mu + \kappa dlr_{t-1}^{NG} + \tau_{t,t}, \\ h_{t,t} &= \psi + \chi \tau_{t,t-1}^2 + \xi h_{t,t-1} + \lambda \sqrt{\hat{h}_{gsb,t-1}}, \end{aligned} \tag{7}$$

and

$$\begin{aligned} dlr_t^{NG} &= \mu + \kappa dlr_{t-1}^{NG} + \tau_{g,t}, \\ h_{g,t} &= \psi + \chi \tau_{g,t-1}^2 + \xi h_{g,t-1} + \lambda \sqrt{\hat{h}_{gsb,t-1}}, \end{aligned} \tag{8}$$

where $\sqrt{\hat{h}_{gsb,t-1}}$ denotes the one-day lagged volatility estimates from our hybrid model (4), and λ is the coefficient. Therefore, the statistically significant positive λ values again mean the predictive power of the volatility estimates from our hybrid model, the AR–GED–SB–GARCH model (4). Note that the remaining notations of models (7)–(8) are the same as those of models (1)–(2).

Results

Table 5 shows the results for the predictive power of our hybrid model estimates. Panel A shows the results for the volatility estimates from the AR–T–SB–GARCH model, and Panel B presents those for the volatility estimates from the AR–GED–SB–GARCH model.

In these two panels, the estimated coefficients, λs, are always statistically significant with positive signs. This indicates that the volatility estimates from our hybrid models, the AR–T–SB–GARCH and the AR–GED–SB–GARCH models, have predictive power for the volatilities (variances) of the nonhybrid AR–T–GARCH and AR–GED–GARCH models.

Table 5 Results for predictive power tests of hybrid GARCH model volatility estimates

Panel A. Predictive power of volatility estimates from the AR–T–SB–GARCH model					
Testing models					
AR–T–GARCH			**AR–GED–GARCH**		
Coefficients	**Estimates**	***p*-value**	**Coefficients**	**Estimates**	***p*-value**
Mean equations					
μ	0.107	0.337	μ	0.108	0.331
κ	−0.032	0.313	κ	−0.033	0.270
Variance equations					
ψ	−17.700***	0.000	ψ	−17.875***	0.000
χ	0.024***	0.009	χ	0.024***	0.009
ξ	−0.936***	0.000	ξ	−0.926***	0.000
λ	12.839***	0.000	λ	12.854***	0.000
ν	21.895*	0.083	k	1.105***	0.000
LL	−2843.249		LL	−2843.914	
Panel B. Predictive power of volatility estimates from the AR–GED–SB–GARCH model					
Testing models					
AR–T–GARCH			**AR–GED–GARCH**		
Coefficients	**Estimates**	***p*-value**	**Coefficients**	**Estimates**	***p*-value**
Mean equations					
μ	0.109	0.329	μ	0.109	0.337
κ	−0.035	0.266	κ	−0.036	0.244
Variance equations					
ψ	−17.543***	0.000	ψ	−17.692***	0.000
χ	0.019**	0.047	χ	0.019*	0.052
ξ	−0.918***	0.000	ξ	−0.911***	0.000
λ	12.747***	0.000	λ	12.762***	0.000
ν	22.546*	0.093	k	1.103***	0.000
LL	−2843.466		LL	−2844.061	

LL: log-likelihood value. ***, **, and * denote the 1%, 5%, and 10% significance levels, respectively

We consider that these new findings mean that volatility estimates from our hybrid GARCH models (3)–(4) lead the volatilities of nonhybrid GARCH models (1)–(2). We thus believe that because of this favorable characteristic, the two hybrid GARCH models well captured the volatility jump of the natural gas futures when the tensions simmered on the Russia–Ukraine border.

Hybrid EGARCH models

Model constructions

This section formulates alternative hybrid volatility estimation models using exponential-form GARCH (Nelson 1991). As before, we employ the Student's *t* distribution or GED errors, and we include the first autoregressive variable in the mean equations of our models.

The base models for building our alternative hybrid models are the following AR–T–EGARCH and AR–GED–EGARCH models:

$$
\begin{aligned}
dlr_t^{NG} &= \mu_e + \kappa_e dlr_{t-1}^{NG} + \tau_{t,t}^e, \\
\ln(h_{t,t}^e) &= \psi_e + \chi_e \frac{|\tau_{t,t-1}^e|}{\sqrt{h_{t,t-1}^e}} + \xi_e \ln(h_{t,t-1}^e),
\end{aligned} \tag{9}
$$

and

$$
\begin{aligned}
dlr_t^{NG} &= \mu_e + \kappa_e dlr_{t-1}^{NG} + \tau_{g,t}^e, \\
\ln(h_{g,t}^e) &= \psi_e + \chi_e \frac{|\tau_{g,t-1}^e|}{\sqrt{h_{g,t-1}^e}} + \xi_e \ln(h_{g,t-1}^e),
\end{aligned} \tag{10}
$$

where $\tau_{t,t}^e$ ($\tau_{g,t}^e$) denotes the Student's t distribution (GED) errors at time t with the distribution parameter ν_e (k_e); and $h_{t,t}^e$ ($h_{g,t}^e$) is the variance to be estimated by model (9) (model (10)) at time t. Further, μ_e denotes the mean equation intercept; κ_e denotes the autoregressive term coefficient; ψ_e is the variance equation intercept; χ_e is the ARCH-term coefficient; and ξ_e is the GARCH-term coefficient.

As before, we construct the hybrid EGARCH models by including structural break effects into models (9) and (10). Our exponential-form hybrid models are the following AR–T–SB–EGARCH and AR–GED–SB–EGARCH models:

$$
\begin{aligned}
dlr_t^{NG} &= \mu_e + \kappa_e dlr_{t-1}^{NG} + \tau_{tsb,t}^e, \\
\ln(h_{tsb,t}^e) &= \psi_e + \chi_e \frac{|\tau_{tsb,t-1}^e|}{\sqrt{h_{tsb,t-1}^e}} + \xi_e \ln(h_{tsb,t-1}^e) + \sum_{i=1}^{n} \phi_{e,i} D_{i,t}^{SB},
\end{aligned} \tag{11}
$$

and

$$
\begin{aligned}
dlr_t^{NG} &= \mu_e + \kappa_e dlr_{t-1}^{NG} + \tau_{gsb,t}^e, \\
\ln(h_{gsb,t}^e) &= \psi_e + \chi_e \frac{|\tau_{gsb,t-1}^e|}{\sqrt{h_{gsb,t-1}^e}} + \xi_e \ln(h_{gsb,t-1}^e) + \sum_{i=1}^{n} \phi_{e,i} D_{i,t}^{SB},
\end{aligned} \tag{12}
$$

where $\tau_{tsb,t}^e$ ($\tau_{gsb,t}^e$) denotes the Student's t distribution (GED) errors in model (11) (model (12)) at time t; $h_{tsb,t}^e$ ($h_{gsb,t}^e$) means the variance to be estimated by model (11) (model (12)) at time t.

Furthermore, $D_{i,t}^{SB}$ denotes the i-th structural break dummy variable and n is the number of the structural breaks as before, and $\phi_{e,i}$ is the coefficient of the i-th break dummy variable. The dummy variable is the same as in models (3) and (4). We also note that including the parameters of fat-tailed distributions, ν_e and k_e, the other notations of models (11) and (12) described above are the same as those of models (9)–(10).

Verifications

Table 6 presents the estimation results of models (9)–(12). Panels A–D present that all the model parameters including the shape parameters of the fat-tailed distribution errors are well estimated. Further, as Panels B and D show, the coefficients of our structural break dummy variables—$\phi_{e,1}$ to $\phi_{e,7}$—are all statistically significant.

Table 6 Estimation results for hybrid EGARCH models

Panel A. AR–T–EGARCH			**Panel B. AR–T–SB–EGARCH**		
Coefficients	**Estimates**	***p*-value**	**Coefficients**	**Estimates**	***p*-value**
Mean equations					
μ_e	0.145	0.200	μ_e	0.110	0.326
κ_e	−0.034	0.278	κ_e	−0.031	0.318
Variance equations					
ψ_e	−0.077***	0.002	ψ_e	1.343***	0.000
χ_e	0.157***	0.000	χ_e	−0.005	0.937
ξ_e	0.985***	0.000	ξ_e	0.498***	0.000
			$\phi_{e,1}$	1.061***	0.005
			$\phi_{e,2}$	−1.027***	0.006
			$\phi_{e,3}$	−0.724***	0.002
			$\phi_{e,4}$	1.006***	0.000
			$\phi_{e,5}$	1.439***	0.001
			$\phi_{e,6}$	−1.395***	0.001
			$\phi_{e,7}$	−0.430***	0.002
ν_e	7.193***	0.000	ν_e	25.260	0.137
LL	−2881.586		LL	−2846.020	
Panel C. AR–GED–EGARCH			**Panel D. AR–GED–SB–EGARCH**		
Coefficients	**Estimates**	***p*-value**	**Coefficients**	**Estimates**	***p*-value**
Mean equations					
μ_e	0.159	0.143	μ_e	0.109	0.324
κ_e	−0.040	0.177	κ_e	−0.033	0.289
Variance equations					
ψ_e	−0.081***	0.001	ψ_e	1.340***	0.000
χ_e	0.158***	0.000	χ_e	−0.018	0.768
ξ_e	0.986***	0.000	ξ_e	0.507***	0.000
			$\phi_{e,1}$	1.046***	0.003
			$\phi_{e,2}$	−1.022***	0.004
			$\phi_{e,3}$	−0.718***	0.000
			$\phi_{e,4}$	0.993***	0.000
			$\phi_{e,5}$	1.428***	0.000
			$\phi_{e,6}$	−1.382***	0.000
			$\phi_{e,7}$	−0.430***	0.000
k_e	1.414***	0.000	k_e	1.093***	0.000
LL	−2888.781		LL	−2846.430	

LL: log-likelihood value. *** denotes the 1% significance level

We note that when incorporating structural breaks, the ARCH effect again disappears (The significant coefficients, χ_e, in Panels A and C of Table 6 become insignificant in Panels B and D.) and the GARCH effect is again weakened (The significant values of the coefficients, ξ_e, in Panels A and C of Table 6 become smaller in Panels B and D.). Therefore, we understand that this again shows the effectiveness of structural breaks in explaining the evolution of natural gas futures volatilities.

Moreover, we performed the LR tests to compare the performance of models (9)–(12) as before, and showed the results in Table 7. As Table 7 indicates, the four null hypotheses—the AR–EGARCH model, which has normal distribution errors,

Table 7 LR tests for EGARCH model discrimination

Panel A. AR–EGARCH vs. AR–T–EGARCH	
$\chi^2(1)$	54.899***
p-value	0.000
Panel B. AR–T–EGARCH vs. AR–T–SB–EGARCH	
$\chi^2(7)$	71.131***
p-value	0.000
Panel C. AR–EGARCH vs. AR–GED–EGARCH	
$\chi^2(1)$	40.509***
p-value	0.000
Panel D. AR–GED–EGARCH vs. AR–GED–SB–EGARCH	
$\chi^2(7)$	84.703***
p-value	0.000

*** denotes the 1% significance level. The test statistic follows a $\chi^2(n)$ distribution with *n* degrees of freedom. The null hypotheses are: the AR–EGARCH model is superior to the AR–T–EGARCH model (Panel A); the AR–T–EGARCH model is superior to the AR–T–SB–EGARCH model (Panel B); the AR–EGARCH model is superior to the AR–GED–EGARCH model (Panel C); the AR–GED–EGARCH model is superior to the AR–GED–SB–EGARCH model (Panel D). AR–EGARCH model has normal distribution errors

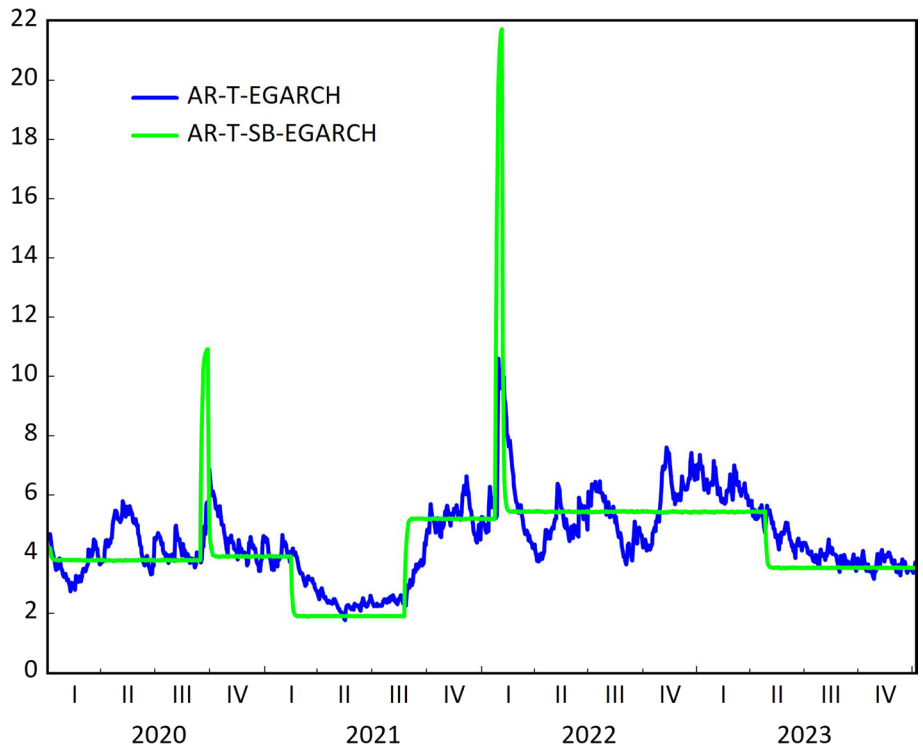

Fig. 6 Estimated daily volatilities from AR–T–EGARCH and AR–T–SB–EGARCH models

is superior to the AR–T–EGARCH model (Panel A), the AR–T–EGARCH model is superior to the AR–T–SB–EGARCH model (Panel B), the AR–EGARCH model is superior to the AR–GED–EGARCH model (Panel C), and the AR–GED–EGARCH

model is superior to the AR–GED–SB–EGARCH model (Panel D)—are all strongly rejected.

Furthermore, the AIC values for models (9)–(12) are 5775.172, 5789.563, 5718.041, and 5718.860, respectively. That is, the LR test results and the AIC values clearly show the superiority of our alternative hybrid models, the AR–T–SB–EGARCH model and the AR–GED–SB–EGARCH model, and prove the effectiveness for taking both non-normal fat-tail errors and structural breaks into consideration in our natural gas futures volatility analyses.

Why are hybrid EGARCHs effective?

This section considers why our hybrid EGARCH models are effective. For this purpose, we plot the volatility estimates from our alternative hybrid models (11) and (12) in Figs. 6 and 7 to compare the model estimates. Specifically, Fig. 6 exhibits the volatility estimates from the AR–T–EGARCH model with those from the AR–T–SB–EGARCH model, and Fig. 7 displays the volatility estimates from the AR–GED–EGARCH model with those from the AR–GED–SB–EGARCH model.

From Figs. 6 and 7, we can see that when volatilities jump, the volatility estimates from the AR–T–SB–EGARCH and the AR–GED–SB–EGARCH models lead the volatility estimates from the AR–T–EGARCH and the AR–GED–EGARCH models, respectively. Considering this and to clarify why our hybrid EGARCH models are effective, we below test whether the volatility estimates from our two hybrid EGARCH models have predictive power for the volatilities of the nonhybrid EGARCH models.

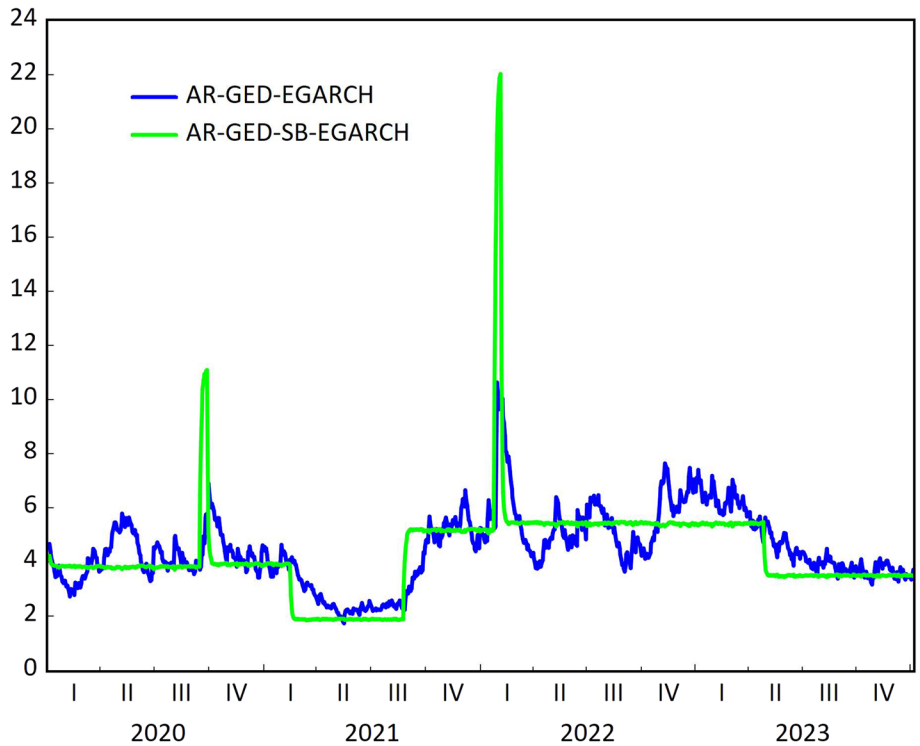

Fig. 7 Estimated daily volatilities from AR–GED–EGARCH and AR–GED–SB–EGARCH models

Testing models

This section examines the forecast power of our hybrid EGARCH model estimates for the nonhybrid EGARCH model volatilities (precisely, variances). Specifically, to test the predictive power of the volatility estimates from the AR–T–SB–EGARCH model (11), we first use the following AR–T–EGARCH–X model with $\sqrt{\hat{h}^e_{tsb,t-1}}$ and the AR–GED–EGARCH–X model with $\sqrt{\hat{h}^e_{tsb,t-1}}$:

$$\begin{aligned} dlr_t^{NG} &= \mu_e + \kappa_e dlr_{t-1}^{NG} + \tau_{t,t}^e, \\ \ln(h_{t,t}^e) &= \psi_e + \chi_e \frac{|\tau_{t,t-1}^e|}{\sqrt{h_{t,t-1}^e}} + \xi_e \ln(h_{t,t-1}^e) + \lambda_e \sqrt{\hat{h}^e_{tsb,t-1}}, \end{aligned} \tag{13}$$

and

$$\begin{aligned} dlr_t^{NG} &= \mu_e + \kappa_e dlr_{t-1}^{NG} + \tau_{g,t}^e, \\ \ln(h_{g,t}^e) &= \psi_e + \chi_e \frac{|\tau_{g,t-1}^e|}{\sqrt{h_{g,t-1}^e}} + \xi_e \ln(h_{g,t-1}^e) + \lambda_e \sqrt{\hat{h}^e_{tsb,t-1}}, \end{aligned} \tag{14}$$

where $\sqrt{\hat{h}^e_{tsb,t-1}}$ denotes the one-day lagged volatility estimates from our hybrid model (11), and λ_e is the coefficient. Hence, the statistically significant positive λ_e values mean the predictive power of the volatility estimates from our hybrid EGARCH model, the AR–T–SB–EGARCH model. Note that the other notations of models (13)–(14) are the same as those of models (9)–(10).

Moreover, also to test the forecast power of the volatility estimates from the AR–GED–SB–EGARCH model (12), we use the following AR–T–EGARCH–X model with $\sqrt{\hat{h}^e_{gsb,t-1}}$ and the AR–GED–EGARCH–X model with $\sqrt{\hat{h}^e_{gsb,t-1}}$:

$$\begin{aligned} dlr_t^{NG} &= \mu_e + \kappa_e dlr_{t-1}^{NG} + \tau_{t,t}^e, \\ \ln(h_{t,t}^e) &= \psi_e + \chi_e \frac{|\tau_{t,t-1}^e|}{\sqrt{h_{t,t-1}^e}} + \xi_e \ln(h_{t,t-1}^e) + \lambda_e \sqrt{\hat{h}^e_{gsb,t-1}}, \end{aligned} \tag{15}$$

and

$$\begin{aligned} dlr_t^{NG} &= \mu_e + \kappa_e dlr_{t-1}^{NG} + \tau_{g,t}^e, \\ \ln(h_{g,t}^e) &= \psi_e + \chi_e \frac{|\tau_{g,t-1}^e|}{\sqrt{h_{g,t-1}^e}} + \xi_e \ln(h_{g,t-1}^e) + \lambda_e \sqrt{\hat{h}^e_{gsb,t-1}}, \end{aligned} \tag{16}$$

where $\sqrt{\hat{h}^e_{gsb,t-1}}$ denotes the one-day lagged volatility estimates from our hybrid EGARCH model (12), and λ_e is the coefficient. Thus, the statistically significant positive λ_e again indicates the predictive power of the volatility estimates from our alternative hybrid model, the AR–GED–SB–EGARCH model. Note that the other notations of models (15)–(16) are the same as those of models (9)–(10).

Table 8 Results for predictive power tests of hybrid EGARCH model volatility estimates

Panel A. Predictive power of volatility estimates from the AR–T–SB–EGARCH model					
Testing models					
AR–T–EGARCH			**AR–GED–EGARCH**		
Coefficients	**Estimates**	***p*-value**	**Coefficients**	**Estimates**	***p*-value**
Mean equations					
μ_e	0.092	0.467	μ_e	0.095	0.422
κ_e	−0.032	0.311	κ_e	−0.033	0.355
Variance equations					
ψ_e	1.500***	0.000	ψ_e	1.511***	0.000
χ_e	0.048	0.413	χ_e	0.043	0.452
ξ_e	−0.611***	0.000	ξ_e	−0.615***	0.000
λ_e	0.695***	0.000	λ_e	0.696***	0.000
ν_e	20.086*	0.057	k_e	1.127***	0.000
LL	−2857.180		LL	−2857.934	
Panel B. Predictive power of volatility estimates from the AR–GED–SB–EGARCH model					
Testing models					
AR–T–EGARCH			**AR–GED–EGARCH**		
Coefficients	**Estimates**	***p*-value**	**Coefficients**	**Estimates**	***p*-value**
Mean equations					
μ_e	0.093	0.432	μ_e	0.095	0.401
κ_e	−0.033	0.301	κ_e	−0.034	0.269
Variance equations					
ψ_e	1.520***	0.000	ψ_e	1.530***	0.000
χ_e	0.041	0.495	χ_e	0.035	0.543
ξ_e	−0.611***	0.000	ξ_e	−0.615***	0.000
λ_e	0.691***	0.000	λ_e	0.693***	0.000
ν_e	20.522*	0.058	k_e	1.126***	0.000
LL	−2857.589		LL	−2858.252	

LL: log-likelihood value. *** and * denote the 1% and 10% significance levels, respectively

Results

Table 8 presents the results for the predictive power of our hybrid EGARCH model estimates. Panel A exhibits the results for the volatility estimates from the AR–T–SB–EGARCH model, and Panel B shows those for the volatility estimates from the AR–GED–SB–EGARCH model.

In these two panels, the estimated coefficients, λ_es, are always statistically significant with positive signs; and thus this means that the volatility estimates from our hybrid EGARCH models, the AR–T–SB–EGARCH and the AR–GED–SB–EGARCH models, have predictive power for the volatilities (variances) of the nonhybrid models, the AR–T–EGARCH and the AR–GED–EGARCH models.

We consider that these new findings mean that volatility estimates from our hybrid EGARCH models (11)–(12) lead the volatilities of nonhybrid EGARCH models (9)–(10). Hence as before, we consider that because of this favorable characteristic, the two hybrid EGARCH models timely captured the volatility spile of the natural gas futures when the tension summered in the Ukraine-Russia border.

Implications and perspectives

This section discusses how we can interpret our results and derive significant implications and perspectives for academic energy research and practical industries in the post-COVID-19 era. As in Ahmed et al. (2022), Chaklader et al. (2023), and Dirican (2015), AI will play a more significant role in various industries in the future. The implications of our study along with the innovative perspectives derived from our research are as follows.

Firstly, as we have demonstrated, to accurately capture the impact of significant events, natural gas futures volatilities should be estimated by incorporating fat-tailed errors and structural breaks. We believe that capturing structural breaks in a timely manner is particularly crucial for volatility modeling and future risk management in the energy markets and industries. This is because, as we found in Figs. 4, 5, 6, and 7, the volatilities derived from nonhybrid models lag behind the volatilities from our four hybrid models, which incorporate structural breaks. The lag is especially evident during the time when tensions simmered on the Russia–Ukraine border. Therefore, it is crucial for us to accurately forecast energy price volatilities without lagging behind significant events by utilizing innovative AI techniques such as machine learning. This will lead to more effective risk management in the energy markets and industries in the post-COVID-19 era.

Secondly, given the increasing importance of structural breaks in energy markets that we have observed, it is now more crucial than ever for us to accurately predict these breaks. We should note that these breaks are caused by information related to the energy markets. We should strive to accurately predict these breaks by using cutting-edge AI technologies. This will improve risk management in the energy markets and industries, particularly in the unpredictable post-COVID-19 world. We also believe that accurately predicting structural breaks allows us to forecast volatilities without falling behind sudden changes in energy prices caused by significant events.

Thirdly, as a policy implication, we suggest that policy makers and energy-related industry practitioners need to pay closer attention not only to the demand and supply balance for energy, but also to various news and its impact on energy market prices, even during normal circumstances. These efforts and close observation should help prevent potential imbalances in energy markets in the future. Furthermore, our results suggest that policy making and risk management in the energy industry should be conducted more swiftly than in the past. This is due to the fact that energy prices now respond more quickly to various events and news than ever before. One deeper interpretation of our results is that market efficiency in energy markets may have shifted. We believe that we should take this viewpoint into consideration in policy making and risk management in the energy industry.

Fourth, an interesting implication for future research would be to utilize machine learning approaches, such as reinforcement learning or deep learning for predicting energy price fluctuations. We consider that comparing traditional econometric models with machine learning approaches in our context would be a valuable direction for future research. We believe that our methods can be applied to other real-world assets, such as fuel and other energy commodities.

While this study does not provide methods for forecasting structural breaks, the comprehensive inspections conducted in this paper provide many insightful interpretations, implications, and innovative perspectives. Collectively, these demonstrate the importance of our current work for future energy research and practice. Therefore, we believe that our empirical findings, along with the significant interpretations, implications, and innovative viewpoints discussed above, all signify our substantial contribution to current and future research on energy informatics.

Contributions and conclusions

Paying keen attention to the Russia–Ukraine war, and particularly its impact on natural gas futures prices when tensions simmered on the Russia–Ukraine border, this paper empirically examined natural gas futures volatilities. Using the four hybrid models, the AR–T–SB–GARCH, the AR–GED–SB–GARCH, the AR–T–SB–EGARCH, and the AR–GED–SB–EGARCH models, which incorporated both fat-tailed errors and structural breaks, we derived the following findings as new contributions.

- First, we found that very interestingly, it was not when Russia invaded Ukraine in February 2022, but rather when tensions on the border simmered in January 2022, that the matter of the Russia–Ukraine war had the most impact on natural gas futures prices.
- Second, we revealed that our hybrid models, not only with fat-tailed errors—Student's t distribution or GED errors—but also with structural breaks, effectively capture the natural gas futures volatility spike when tensions on the Russia–Ukraine border simmered in January 2022.
- Third, we also uncovered that our hybrid modeling approach—incorporating both fat-tailed errors and structural breaks—is highly effective, not only in GARCH models but also in EGARCH models. This demonstrates the robustness of the effectiveness of our hybrid modeling approach in capturing natural gas futures volatilities.
- Fourth, we also newly found that the volatility estimates from our hybrid models of the AR–T–SB–GARCH and the AR–GED–SB–GARCH models have predictive power for the volatilities of nonhybrid AR–T–GARCH and AR–GED–GARCH models. We consider that because of this beneficial characteristic, our hybrid GARCH models well captured the natural gas futures volatility jump when the tensions on the Russia–Ukraine border simmered.
- Fifth, we also uncovered that the volatility estimates from our exponential-form hybrid models of the AR–T–SB–EGARCH and the AR–GED–SB–EGARCH models also have forecast power for the volatilities of nonhybrid AR–T–EGARCH and AR–GED–EGARCH models. This indicates the robustness of the predictive power, and again, we suggest that because of this characteristic, our hybrid EGARCH models also timely captured the natural gas futures volatility spike when the tensions in Russia–Ukraine border simmered.
- Sixth, we further elucidated that the evidence of the predictive power of our hybrid models for the volatilities of nonhybrid models means that the volatility estimates from the nonhybrid models lag behind the volatilities of the hybrid models. We con-

sider that because of this characteristic, the nonhybrid models are inferior to the hybrid models in capturing sudden changes in natural gas futures volatilities.

- Seventh, in addition to the above, we have also developed and shared numerous valuable interpretations, implications, and innovative perspectives for future risk management, policy-making practices, and related research in energy informatics. This represents another significant contribution of our work. These interpretations, implications, and innovative perspectives, wihch include the effective use of AI, should be valuable not only for academic researchers but also for industry practitioners.

This study examined the impact of war as a manmade disaster on natural gas futures prices, which is of great importance for research in energy informatics. Additionally, the findings from our study indicate the growing significance of structural breaks in energy markets. This highlights the need to closely monitor the immediate news impact on contemporary energy markets.

As a broader implication for future research, studies that explore similar models in different energy-related markets or under various geopolitical scenarios would be interesting. Further research into the adaptability and scalability of the proposed hybrid models in our current study would provide a pathway for ongoing contributions in the field of energy informatics. Given this, we believe that the many new findings derived from our present study make a significant contribution not only to the body of academic energy informatics research but also to actual practice in energy-related industries.

Acknowledgements
The author appreciates Zheng Grace Ma (Editor-in-Chief) for her skillful editorship of this paper. The author thanks two anonymous reviewers for their supportive comments on this paper.

Author contributions
The author conducted all the research and wrote the entire manuscript.

Funding
This work was supported by the Chuo University Grant for Special Research.

Data availibility
Not applicable.

Declarations

Ethical approval and consent to participate
Not applicable.

Consent for publication
Not applicable.

Competing interests
The author declares no conflicts of interest.

Received: 7 April 2024 Accepted: 2 May 2024
Published online: 14 May 2024

References

Ahmed S, Alshater MM, Ammari AE, Hammami H (2022) Artificial intelligence and machine learning in finance: a bibliometric review. Res Int Bus Financ 61:101646

Akcora B, Kocaaslan OK (2023) Price bubbles in the European natural gas market between 2011 and 2020. Resour Pol 80:103186

Bian Z, Meng X, Tao M, Lv Y, Xin Z (2016) Effect of MoO_3 on catalytic performance and stability of the SBA-16 supported Ni-catalyst for CO methanation. Fuel 179:193–201

Chaklader B, Gupta BB, Panigrahi PK (2023) Analyzing the progress of FINTECH-companies and their integration with new technologies for innovation and entrepreneurship. J Bus Res 161:113847
Chalkidis A, Jampaiah D, Hartley PG, Sabri YM, Bhargava SK (2019) Regenerable α-MnO_2 nanotubes for elemental mercury removal from natural gas. Fuel Process Technol 193:317–327
Chen G, Yang S, Wei F, Zhang K, Nie D, Gong H (2023) Effects of operating parameters on combustion and soot emissions in a pilot ignited HPDI natural gas engine for different combustion modes. Fuel 337:127160
Cisneros S, Chen S, Diemant T, Bansmann J, Abdel-Mageed AM, Goepel M, Olesen SE, Welter ES, Parlinska-Wojtan M, Gläser R, Chorkendorff I, Behm RJ (2021) Effects of SiO_2-doping on high-surface-area Ru/TiO_2 catalysts for the selective CO methanation. Appl Catal B 282:119483
CNN January 27, 2022 Tensions simmer in Ukraine-Russia border crisis
Dastan SA (2023) The predicaments of the Turkish natural gas market between supply shortages and price hikes. Resour Pol 82:103566
Ding Y-L, Xu C-G, Yu Y-S, Li X-S (2017) Methane recovery from natural gas hydrate with simulated IGCC syngas. Energy 120:192–198
Dirican C (2015) The impacts of robotics, artificial intelligence on business and economics. Procedia Soc Behav Sci 195:564–573
Dutta A, Bouri E, Saeed T, Vo XV (2021) Crude oil volatility and the biodiesel feedstock market in Malaysia during the 2014 oil price decline and the COVID-19 outbreak. Fuel 292:120221
Fan Y, Zhang YJ, Tsai HT, Wei YM (2008) Estimating 'Value at Risk' of crude oil price and its spillover effect using the GED-GARCH approach. Energy Econ 30:3156–3171
Gambelli AM, Rossi F (2019) Natural gas hydrates: comparison between two different applications of thermal stimulation for performing CO_2 replacement. Energy 172:423–434
Geweke J (1993) Bayesian treatment of the independent Student-t linear model. J Appl Econom 8:S19–S40
Guban D, Muritala IK, Roeb M, Sattler C (2020) Assessment of sustainable high temperature hydrogen production technologies. Int J Hydrogen Energy 45:26156–26165
Inclán C, Tiao GC (1994) Use of cumulative sums of squares for retrospective detection of changes of variance. J Am Stat Assoc 89:913–923
Ji M, Wang J (2021) Review and comparison of various hydrogen production methods based on costs and life cycle impact assessment indicators. Int J Hydrogen Energy 46:38612–38635
Jingjian S, Xiangyun G, Jinsheng Z, Anjian W, Xiaotian S, Yiran Z, Hongyu W (2023) The impact of oil price shocks on energy stocks from the perspective of investor attention. Energy 278:127987
Ju K, Zhou D, Zhou P, Wu J (2014) Macroeconomic effects of oil price shocks in China: an empirical study based on Hilbert-Huang transform and event study. Appl Energy 136:1053–1066
Kim W, Park C, Bae C (2021) Characterization of combustion process and emissions in a natural gas/diesel dual-fuel compression-ignition engine. Fuel 291:120043
Koh D-Y, Kang H, Lee J-W, Park Y, Kim S-J, Lee J, Lee JY, Lee H (2016) Energy-efficient natural gas hydrate production using gas exchange. Appl Energy 162:114–130
Koulocheris V, Louli V, Panteli E, Skouras S, Voutsas E (2018) Modelling of elemental mercury solubility in natural gas components. Fuel 233:558–564
Koulocheris V, Louli V, Panteli E, Voutsas E (2023) Simulation of mercury distribution in an offshore natural gas processing platform. Fuel 345:128164
Li W, Ma J, Liu H, Wang H, Zhang H, Qi T, Wu D, Pan J (2023) Investigations on combustion system optimization of a heavy-duty natural gas engine. Fuel 331:125621
Liu SS, Jin YY, Han Y, Zhao J, Ren J (2018a) Highly stable and coking resistant Ce promoted Ni/SiC catalyst towards high temperature CO methanation. Fuel Process Technol 177:266–274
Liu Y, Hou J, Zhao H, Liu X, Xia Z (2018b) A method to recover natural gas hydrates with geothermal energy conveyed by CO_2. Energy 144:265–278
Liu H, Pata UK, Zafar MW, Kartal MT, Karlilar S, Caglar AE (2023) Do oil and natural gas prices affect carbon efficiency? Daily evidence from China by wavelet transform-based approaches. Resour Pol 85:104039
Malik F (2022) Volatility spillover among sector equity returns under structural breaks. Rev Quant Financ Account 58:1063–1080
Mensi W, Selmi R, Al-Kharusi S, Belghouthi HE, Kang SH (2024) Connectedness between green bonds, conventional bonds, oil, heating oil, natural gas, and petrol: new evidence during bear and bull market scenarios. Resour Pol 91:104888
Nelson DB (1991) Conditional heteroskedasticity in asset returns: a new approach. Econometrica 59:347–370
Olabi AG, Bahri AS, Abdelghafar AA, Baroutaji A, Sayed ET, Alami AH, Rezk H, Abdelkareem MA (2021) Large-vscale hydrogen production and storage technologies: current status and future directions. Int J Hydrogen Energy 46:23498–23528
Pontes FVM, Carneiro MC, Vaitsman DS, Monteiro MIC, Neto AA, Tristão MLB (2014) Investigation of the Grignard reaction and experimental conditions for the determination of inorganic mercury and methylmercury in crude oils by GC-ICP-MS. Fuel 116:421–426
Puig-Gamero M, Trapero JR, Pedregal DJ, Sánchez P, Sanchez-Silva L (2021) Impact of the forecast price on economic results for methanol production from olive waste. Fuel 295:120631
Qureshi F, Yusuf M, Pasha AA, Khan HW, Imteyaz B, Irshad K (2022) Sustainable and energy efficient hydrogen production via glycerol reforming techniques: a review. Int J Hydrogen Energy 47:41397–41420
Sanusi YS, Mokheimer EMA (2019) Thermo-economic optimization of hydrogen production in a membrane-SMR integrated to ITM-oxy-combustion plant using genetic algorithm. Appl Energy 235:164–176
Shen F, He S, Li J, Wang P, Liu H, Xiang K (2023) Novel insight into elemental mercury removal by cobalt sulfide anchored porous carbon: phase-dependent interfacial activity and mechanisms. Fuel 331:125740
Su CW, Qin M, Chang HL, Ţăran AM (2023) Which risks drive European natural gas bubbles? Novel evidence from geopolitics and climate. Resour Pol 81:103381

Tao M, Meng X, Lv Y, Bian Z, Xin Z (2016) Effect of impregnation solvent on Ni dispersion and catalytic properties of Ni/SBA-15 for CO methanation reaction. Fuel 165:289–297
Tao M, Xin Z, Meng X, Bian Z, Lv Y (2017) Highly dispersed nickel within mesochannels of SBA-15 for CO methanation with enhanced activity and excellent thermostability. Fuel 188:267–276
Thiruvengadam A, Besch M, Padmanaban V, Pradhan S, Demirgok B (2018) Natural gas vehicles in heavy-duty transportation-a review. Energ Policy 122:253–259
Tsuji C (2018) New DCC analyses of return transmission, volatility spillovers, and optimal hedging among oil futures and oil equities in oil-producing countries. Appl Energy 229:1202–1217
Tsuji C (2020) New evidence on dynamic interactions between biofuel crops, crude oil, and US and European equities—a quinquevariate approach. Fuel 277:117765
Tupsakhare SS, Castaldi MJ (2019) Efficiency enhancements in methane recovery from natural gas hydrates using injection of CO_2/N_2 gas mixture simulating in-situ combustion. Appl Energy 236:825–836
Tutak W, Jamrozik A, Grab-Rogaliński K (2020) Effect of natural gas enrichment with hydrogen on combustion process and emission characteristic of a dual fuel diesel engine. Int J Hydrogen Energy 45:9088–9097
van Eyden R, Difeto M, Gupta R, Wohar ME (2019) Oil price volatility and economic growth: evidence from advanced economies using more than a century's data. Appl Energy 233–234:612–621
Wang P, Moore T (2009) Sudden changes in volatility: the case of five central European stock markets. J Int Financ Mark, Inst & Money 19:33–46
Wang J, Wang J, Zhang Y, Wang T, Pan W-P (2020) Ionic mercury captured by H_2S sulfurized biochar in liquid hydrocarbons: mechanism and stability evaluation. Fuel 278:118413
Wang Z, Zhang F, Xia Y, Wang D, Xu Y, Du G (2021) Combustion phase of a diesel/natural gas dual fuel engine under various pilot diesel injection timings. Fuel 289:119869
Wang Y, Li H, Altuntaş M (2022) Volatility in natural resources commodity prices: evaluating volatility in oil and gas rents. Resour Pol 77:102766
Wei L, Geng P (2016) A review on natural gas/diesel dual fuel combustion, emissions and performance. Fuel Process Technol 142:264–278
Xu C-G, Cai J, Yu Y-S, Chen Z-Y, Li X-S (2018a) Research on micro-mechanism and efficiency of CH_4 exploitation via CH_4-CO_2 replacement from natural gas hydrates. Fuel 216:255–265
Xu C-G, Cai J, Yu Y-S, Yan K-F, Li X-S (2018b) Effect of pressure on methane recovery from natural gas hydrates by methane-carbon dioxide replacement. Appl Energy 217:527–536
Younas M, Shafique S, Hafeez A, Javed F, Rehman F (2022) An overview of hydrogen production: current status, potential, and challenges. Fuel 316:123317
Zhang Q, Guo X, Yao X, Cao Z, Sha Y, Chen B, Zhou H (2020) Modeling, simulation, and systematic analysis of high-temperature adiabatic fixed-bed process of CO methanation with novel catalysts. Appl Energy 279:115822
Zhou Z, Liu X, Li C, Cao XE, Xu M (2020) Seawater-assisted synthesis of MnCe/zeolite-13X for removing elemental mercury from coal-fired flue gas. Fuel 262:116605
Zhu H, Xu T, Yuan Y, Xia Y, Xin X (2020) Numerical investigation of the natural gas hydrate production tests in the Nankai Trough by incorporating sand migration. Appl Energy 275:115384

Publisher's Note